REVISTA BRASILEIRA DE AGRICULTURA IRRIGADA

Revista Brasileira de Agricultura Irrigada v.13, nº.3, p. 3421 - 3434, 2019
ISSN 1982-7679 (On-line)
Fortaleza, CE, INOVAGRI – http://www.inovagri.org.br
DOI: 10.7127/rbai.v13n301040
Protocolo 1040.19 – 15/11/2018   Aprovado em 06/04/2019

ESTIMATION OF THE REAL EVAPOTRANSPIRATION WITH REFINEMENT OF THE LANDSAT THERMAL IMAGE BAND

Antônio Erivando Bezerra[1], Carlos Wagner Oliveira[2], Johny de Souza Silva[3], Ana Célia Maia Meireles[4], Toshik Iarley da Silva[5], João Miguel de Moraes Neto[6]

ABSTRACT

Irrigated agricultural activity is responsible for large food production, however it is pointed out as the major consumer of water. To compute the real evapotranspiration by means of remote sensing, short-wave images with spatial resolution of 30m x 30m "pixel" (Landsat) are used. While the images with long wave bands (thermal) have a resolution between 60m x 60m and 120m x 120m, which compromise the result. This work proposes the improvement of the spatial resolution of the actual evapotranspiration obtained by energy balance, using the METRIC model, by improving the spatial resolution of the thermal band used. The refinement of the thermal band allows a better visualization and spatialization of evapotranspiration values. Therefore, the refinement of the thermal band is an extremely important tool for the estimation of the real evapotranspiration values in agricultural areas, considerably improving the spatial resolution of the images (up to 16 times), corroborating with activities related to the environmental scope, water resources management and agriculture.
Keywords: remote sensing, energy balance, METRIC.

ESTIMATIVA DA EVAPOTRANSPIRAÇÃO REAL COM REFINAMENTO DA BANDA TÉRMICA DE IMAGENS LANDSAT

RESUMO

A agricultura irrigada apesar de ser apontada como o setor de maior consumo de água é responsável pela maior produção de alimentos. Para computo da evapotranspiração real por meio de sensoriamento remoto, pode-se utilizar, por exemplo, imagens do satélite Landsat, com bandas de comprimento de ondas curtas, com resolução espacial de 30m x 30m “pixel”. Enquanto as imagens com bandas de onda longa (termais) apresentam resolução entre 60m x 60m e 120m x 120m, as quais comprometem o resultado. Este trabalho se propõe melhorar a resolução espacial da evapotranspiração real obtido por balanço de energia, utilizando o modelo METRIC, através da melhoria da resolução espacial da banda

[1] Mestre em Engenharia Agrícola, UFCG, Campina Grande-PB, e-mail: aerivando86@gmail.com
[2] PhD em Biosystems Engineering, Professor da UFCA, Crato-CE, e-mail: carlos.oliveira@ufca.edu.br
[3] Mestrando em Fitotecnia, UFC, Fortaleza-CE, e-mail: johny.ufca@gmail.com
[4] Doutora em Engenharia Civil (Recursos Hídricos), Professora da UFCA, Crato-CE, e-mail: ana.meireles@ufca.edu.br
[5] Doutorando em Fitotecnia, UFV, Viçosa-MG, e-mail: iarley.toshik@gmail.com
[6] Doutor em Recursos Naturais, Professor da UFCG, Campina Grande-PB, e-mail: moraes@deag.ufcg.edu.br

térmica utilizada. O refinamento da banda térmica permitiu uma melhor visualização e espacialização dos valores de evapotranspiração. Portanto, o refinamento da banda térmica apresenta-se como ferramenta de extrema relevância para realização de estimativa dos valores de evapotranspiração real em áreas agrícolas, melhorando consideravelmente em até 16 vezes a resolução espacial das imagens, corroborando com atividades direcionadas ao âmbito ambiental, gestão dos recursos hídricos e agricultura.

Palavras-chave: sensoriamento remoto, balanço energia, METRIC.

INTRODUCTION

The rational use of water in irrigated agriculture should be considered a priority goal since water consumption by the agricultural sector is very high, representing about 70% of the water available in rivers, lakes and aquifers (EBC, 2016). To perform an estimated water demand of a culture, it is necessary to know in details the components of the hydrological cycle, particularly evapotranspiration once, that it is strongly influenced by the type of vegetation, agricultural management, environmental management, and mainly by climatic parameters, including solar radiation, wind, temperature, and relative humidity (ALLEN et al., 2010).

Obtaining reliable information at low cost and on evapotranspiration through remote sensing and modeling is quite relevant, and preferably to be acquired in field scale or subfield (ZHOU et al., 2016). Thus, the fine resolution satellite imagery such as Landsat series of satellites and ET maps that can be generated from them, in addition to derivatives are highly desirable (ALLEN et al., 2008).

The algorithm Mapping Evapotranspiration at High Resolution and with Internalized Calibration (METRIC) is presented as an improvement over the SEBAL model (BASTIAANSSEN et al., 2005), to estimate evapotranspiration (ETR) of a culture using the residual of equation energy balance (ALLEN et al., 2010).

Because the model is applied pixel by pixel, the spatial resolution of ETr map is directly determined by the spatial resolution of short wave and long channels of the images generated by optical and thermal sensors (ARAÚJO et al., 2012). This type of model has been used successfully in diverse ecosystems being agriculture or in areas with native vegetation (MACHADO et al., 2014; SPILIOTOPOULOS et al., 2017). A relevant obstacle for the use of remote sensing for monitoring agricultural areas is the low resolution of the thermal band images since it presents a spatial resolution four times lower compared with the bands of the visible and near infrared. This difference tends to hinder the recognition of an area of interest with dimensions equal to or less than film pixel thermal band.

The occurrence of mismatch between the digital data and the actual conditions of the vegetation in the area of interest is a result of the pixel construction process, considering that for the formation of these pixels radiometric information contaminated are used from neighboring areas, thus affecting the calculation of energy balance and consequently the evaporation elements in areas with reduced dimensions (KUSTAS et al., 2003; ALLEN et al., 2007). Disability related to contamination of pixels, outstanding the distorting effects resulting from the use of the thermal band images with lower spatial resolution can be minimized as long as it is adopted a technique of refinement (Sharpening) of the thermal band (ALLEN et al., 2010). This technique consists of correlating the variables Differential Vegetation Index Normalized (NDVI) and surface radiometric temperature (Ts) to obtain a Ts image with a fine spatial resolution similar as the bands of the visible used in the manufacture of vegetation index. Thus, the images provided by the thermal sensors may be used to obtain extremely valuable information such as mapping of the surface energy flow and evapotranspiration, without reducing the accuracy (ARAUJO et al., 2012). The following paper aims to achieve the refinement of the thermal band, based on the correlation between NDVI and Ts variables to generate a new image of Ts with spatial resolution of 30m x 30m pixels, and it is the same used in the calculation of energy balance and evapotranspiration elements of image production with fine spatial resolution.

MATERIAL AND METHODS

To conduct the survey there were chosen the main agricultural areas irrigated in the state of Ceará, in which are produced much of the irrigated agricultural production for domestic consumption and export: District of Irrigation Jaguaribe-Apodi (DIJA), District of Irrigation Tabuleiro Russas (DISTAR), and in District of Irrigation and Baixo Acaraú (DIBAU).

According to Caitano et al. (2011), areas of research vinterest DIJA and DISTAR are on climate semi-arid and DIBAU are on Aw', in the state of Ceará has three types of climate: BSw'h, Aw' and Cw ', with a predominance in approximately 80% of BSw'h (semiarid region), with the rainy season occurring between the months of January to April (Figure 1).

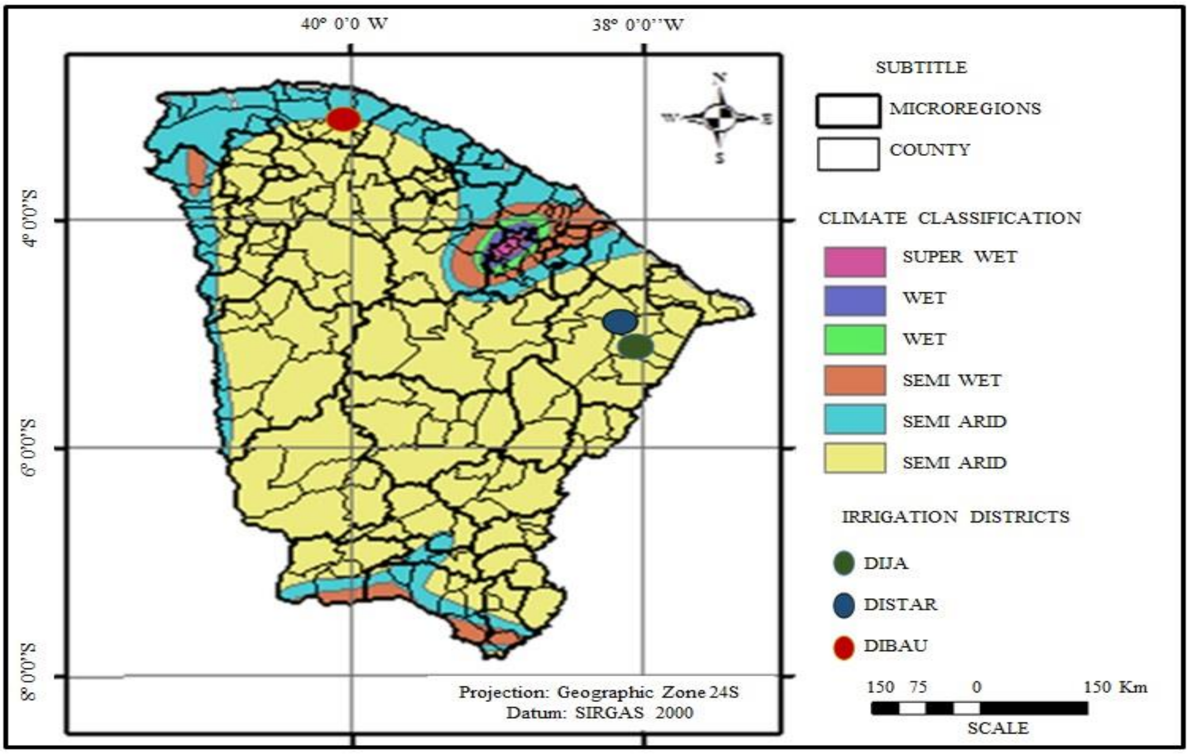

Figure 1. Map of distribution climatic for Ceará, highlighting the location of the irrigated perimeters District of Irrigation Jaguaribe-Apodi (DIJA), District of Irrigation Tabuleiro Russas (DISTAR) e District of Irrigation and Baixo Acaraú D (IBAU).

The estimation of actual evapotranspiration obtained by energy balance using the METRIC model began after obtaining, stacking, orthorectification of satellite images Landsat 5/TM, including the images of the thermal infrared (TIR) acquired at the USGS site (United States Geological Survey) in the "Earth Explorer" platform, with the same excellent source of data for monitoring events occurring in the Earth's surface since the images are provided at no cost to the scientific community (CLAVERIE et al., 2015). The scenes used for characterization of irrigated areas are the orbits and points 218/62 (DIBAU) and 216/64 (DIJA and DISTAR) imaged on the dates 6 and 8 of August 2006, respectively. The choice to work with these images because of its low cloud cover. To facilitate the location of each scene, it was defined the coordinate central, with latitude 5°12'35.62" South, 38°0'36.19" West for (DIJA), longitude 5° 1'34.50" South, 38°

7'14.66" West for (DISTAR) and longitude 3° 5'34.14"S South, 40° 4'28.96"O West for (DIBAU) respectively.

In METRIC procedures it is required a tabular data from automated meteorological data collection platform (DCP's), obtained in parallel form the images, requiring data from at least one station, close to the hot and cold spots within the selected image area (ALLEN et al. 2010). The meteorological data were collected on the website of the National Institute of Meteorology-INMET), the station Apodi being used for DIJA and DISTAR, and Acaraú for DIBAU (INMET, 2014). According to Coelho et al. (2018), NDVI is presented as an index indicative of the amount of biomass produced by the plant and chlorophyll, and its value may vary due to a possible water stress to which the culture is subjected. The calculation is performed based on an equation (TUKER, 1979). The Ts may be obtained by reverse Plank equation, since the emissivity values have been estimated and the gray level values of the thermal image band have been converted to temperature values (CHANDER et al., 2009).

The values of NDVI and Ts were used to perform the refinement of the thermal band, and to generate a new image of Ts_Refined, used in calculation of the elements of energy balance, and refined estimation of actual evapotranspiration were obtained using equations 1 , 2 and 3.

$$\mathrm{NDVI} = \frac{(\rho\mathrm{nir} - \rho\mathrm{red})}{(\rho\mathrm{nir} + \rho\mathrm{red})} \tag{1}$$

$$\mathrm{Ts} = \frac{\mathrm{K_2}}{\ln\left(\frac{\mathrm{K_1}}{\mathrm{L_a}} + 1\right)} \tag{2}$$

$$\mathrm{L_a} = (0{,}0056322 \times \mathrm{DN}) + 0{,}1238 \tag{3}$$

On what:

ρnir: near infrared reflectance; ρred: red reflectance.

Ts: surface temperature in Kelvin; K1 and K2: calibration constants are 607.76 Wm^{-2} sr^{-1} μm^{-1} and 1260.56 Kelvin, respectively; La: Spectral Radiance Band 6 TM sensor, Wm^{-2} sr^{-1} μm^{-1}; DN: digital number. The Ts_refined values were obtained by linear regression containing coefficients which indicate the interception points and straight decline, respectively in relation to the y axis. The coefficients were calculated from the relationship between Ts and NDVI values, with reference to two points, one being indicative of "hot pixel" and the other "cold-pixel", equations 4 and 5, respectively.

The line has a negative sense since the relationship between the variables is inversely proportional, as demonstrated in the equation 6. Solving 4 and 5 to find a and b:

$$\mathrm{ts_{hot\ pixel}} = \mathrm{a} - \mathrm{b.\,NDVI_{hot\ pixel}}$$
$$-\mathrm{ts_{cold\ pixel}} = -\mathrm{a} + \mathrm{b.\,NDVI_{cold\ pixel}}$$
$$\mathrm{ts_{hot\ pixel}} - \mathrm{ts_{cold\ pixel}} = \mathrm{b.\,NDVI_{cold\ pixel}} - \mathrm{b.\,NDVI_{hot\ pixel}}$$
$$\mathrm{ts_{hot\ pixel}} - \mathrm{ts_{cold\ pixel}} = \mathrm{b.\,(NDVI_{cold\ pixel}} - \mathrm{b.\,NDVI_{hot\ pixel})}$$

$$\mathrm{ts_{hot\ pixel}} = \mathrm{a} - \mathrm{b.\,NDVI_{hot\ pixel}} \tag{4}$$

$$\mathrm{ts_{cold\ pixel}} = \mathrm{a} - \mathrm{b.\,NDVI_{cold\ pixel\ (-1)}} \tag{5}$$

$$b = \frac{ts_{\text{hot pixel}} - ts_{\text{cold pixel}}}{NDVI_{\text{cold pixel}} - NDVI_{\text{hot pixel}}} \tag{6}$$

.

$$a = ts_{\text{hot pixel}} + \frac{ts_{\text{hot pixel}} - ts_{\text{cold pixel}}}{NDVI\text{cold pixel} - NDVI_{\text{hot pixel}}} . NDVI_{\text{hot pixel}} \tag{7}$$

.

$$\text{Ts\_Refined} = a + b.\,NDVI \tag{8}$$

1) When the NDVI value is greater than 0.1 is used the regression equation 8.

On what:
Ts_refined: Surface temperature after the thermal refining band, Kelvin; NDVI: normalized differential vegetation index and b: coefficients adjustments, equations 6 and 7.

2) When the NDVI value is less than 0.1, it was decided to repeat the value of the surface temperature since under these conditions, the relationship between NDVI and Ts is very low (equation 9). The identified point may be treated in a body of water or bare soil area with high humidity due to rainfall or irrigation.

$$Ts\text{\_Refined} = Ts \tag{9}$$

On what:
Ts_refined: Surface temperature after the thermal refining band, K; Ts: surface temperature, Kelvin.

Once the elevation has a direct influence on the variation of surface temperature, and this effect can come to mask the air cooling caused by evaporation of water, a temperature adjustment was proposed in relation to altitude, using the elevation model land (Digital elevation Model, DEM), and considering the increase in relation to a base point of a weather station in this image of the scene obtained by the satellite, according to equation 10.

$$\text{Ts\_DEM} = \text{ts} + adjustment \tag{10}$$

$$\text{adjustment} = \text{taxa1\_pln} . \frac{(Z - \text{Z\_base})}{1000} \qquad \text{para } z \leq \text{z\_elev}$$

$$\text{adjustment} = \left[\text{taxa1}_{\text{pln}} . \frac{(Z_{\text{elev}} - Z_{\text{base}})}{1000}\right] + \left[\text{taxa1\_pln} . \frac{(Z - \text{Z\_elev})}{1000}\right] \quad \text{para } z > \text{z\_elev}$$

On what
Ts_DEM: Surface Temperature corrected for terrain elevation, Kelvin; Ts: surface temperature, Kelvin; taxa1_pln: Temperature variation rate for flat areas of the image, considering the amount of 6.5 Kelvin $1000m^{-1}$; taxa2_mnt: Temperature variation rate for mountainous areas of the image, considering the value of 10 Kelvin $1000m^{-1}$; Z: raising the value of each pixel of the image, m; Z_base: arbitrary value in the image where the TS would be equal to the value of ts_DEM, m; Z_elev: Lifting value where there is a change of plan fees for mountainous, m.

The energy balance calculation is performed in sequential steps being terminated when the latent heat flux (LET) is put in evidence, as described in equation 11.

$$\text{LET} = \text{Rn} - \text{Go} - \text{H} \tag{11}$$

On what:

LET: latent heat flow, Wm^{-2}; Rn: radiation balance, Wm^{-2}; G: heat flow in soil; Wm^{-2}; H: sensible heat flux, Wm^{-2}. Equations 12, 13 and 14 demonstrates how it was performed the calculation of the evapotranspiration fraction ETrf; the procedure consists of the division between the values obtained in the evaporation image tracking time (ETinst) by the value of the instantaneous reference evapotranspiration (ET_0inst).

The calculation ET_{0inst} was carried out in Ref-ET software (Allen, 2010) through the Penman-Monteith FAO, using tabular data provided by the nearest weather station.

$$ET_{rf} = \frac{ET_{inst}}{ET_{0inst}} \tag{12}$$

$$ET_{inst} = 3600\,\frac{LET}{\lambda} \tag{13}$$

$$\lambda = [2{,}501 - 0{,}00236\,(T_s - 273)]\ x\ 10^6 \tag{14}$$

On what:

ETrf: evapotranspiration fraction instant measured in each pixel of the image, this value is dimensionless and equals the Kc of the culture; ETinst: Evapotranspiration at the time of image tracking, mm h^{-1}; ETоinst: instantaneous reference evapotranspiration, mm h^{-1}; λ: Latent heat of vaporization of water, J kg^{-1}.

RESULTS AND DISCUSSION

The NDVI images and Ts of irrigated perimeters (DIJA, DISTAR and DIBAU) can identify different situations but with a very similar ratio (Figure 2). Locations with intense green color were highlighted to stand out the occurrence of the maximum NDVI values between 0.5 and 1.0 indicating the massive presence of native or intensive irrigated agriculture vegetation, such as the areas irrigated with central pivot DIJA (Figure 2A) and DIBAU (Figure 2E). On the other hand, the locations with slight vegetation or bare soil present NDVI values between 0.0 and 0.5, which means low to very low colorations were assigned between the magenta and white, respectively. Images of Ts of the locations under analysis show spatial resolution of 120 m x 120 m pixel and a rough visual quality, compromising the identification of irrigated areas or any other area of interest. In the images we can identify only a few spots of blue color as indicative of the occurrence of mild temperatures and others in red being indicative of occurrence of higher temperatures, as can be seen in Figure 2B, Figure 2D and Figure 2F. The temperature varied between 290 and 315 Kelvin, or 23 and 42 °C, respectively.

By correlating the variables in question it can be seen that the smallest Ts values were observed in locations with higher vegetation index, mainly covering the areas with intensive irrigated agriculture. Regarding the reverse situation, it occurs in image points that had low vegetation index.

This assumption reinforces the existence of a strong negative correlation between the variables as described by (ALLEN et al., 2011). Based on the correlation between the surface temperature and vegetation index of the soil of each irrigated area, it became possible to define the linear regression equations and the indication of the adjustment coefficients needed to improve the spatial and distribution of surface temperature values at each location.

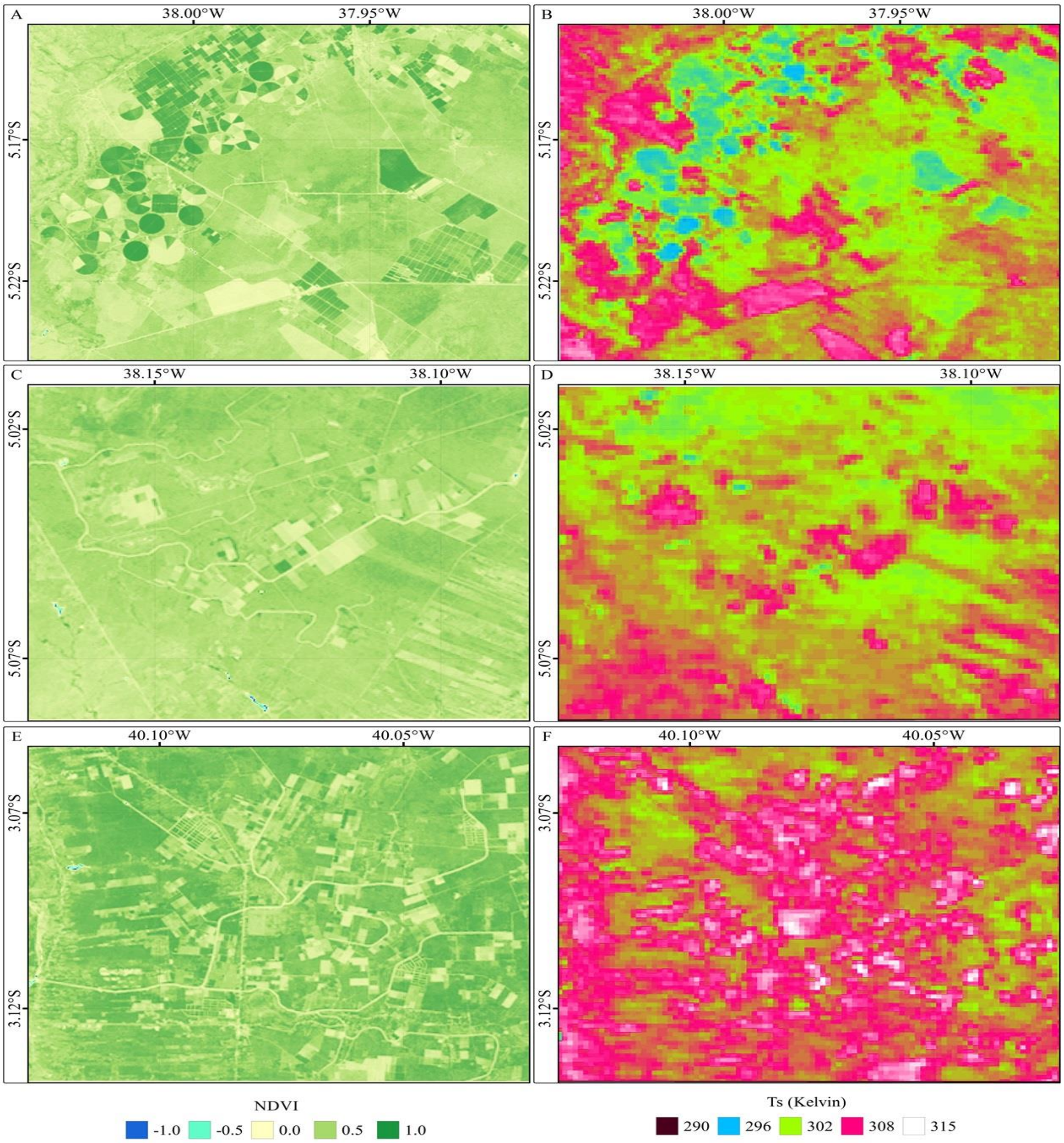

Figure 2. NDVI images with spatial resolution of 30m x 30m pixel and Ts with spatial resolution of 120 x 120m the pixel for the scenes of DIJA-A and B, DISTAR-C and D, DIBAU-E and F, for the dates August of 6 and 8, 2006.

To perform the adjustment two different points indicative of hot pixel (NDVI low and high TS) and cold pixel (high and low NDVI Ts) within the area observed in the image were taken as reference. Due to the soil and climatic characteristics of each area, the regression equations showed different values (Table 1).

Table 1. Established correlation between NDVI x Ts for the scenes corresponding to the areas of DIJA, DISTAR and DIBAU, for the dates 6 and 8 of August, 2006.

Irrigation district	a	b
DIJA	309.97	-16.147
DISTAR	311.13	-14.426
DIBAU	316.75	-19.748

After the model processing, it became notorious the improvement in spatial resolution quality of Ts images, as shown in (Figure 3). Based on the values described in the histogram it can be seen that the frequency distribution of values Ts_Refined is faithfully consistent with the displayed scene (Figure 5). The Ts_Refined of irrigated perimeters of DIJA (Figure 3B), DISTAR (Figure 3D) and DIBAU (Figure 3F) images have similar situations where it was noted the occurrence of small changes, with a reduction of the minimum values and increase in maximum and average values.

Nevertheless, great variations were not found on surface temperature values when compared to Ts and Ts_Refined pictures, considering that the refinement eliminate only the distortion or contamination present in Ts image pixels with a spatial resolution of 120 x 120m allowing the separate analysis of temperature values in different areas of the image even though they exhibit reduced dimensions.

From the frequency histogram analysis and distribution of Ts and ETrf regarding the picture DIJA (Figure 5A), it was perceived little variations, with an increase of the minimum and average values and reduction of the maximum values for Ts_Refined compared to Ts obtained in conventional manner.

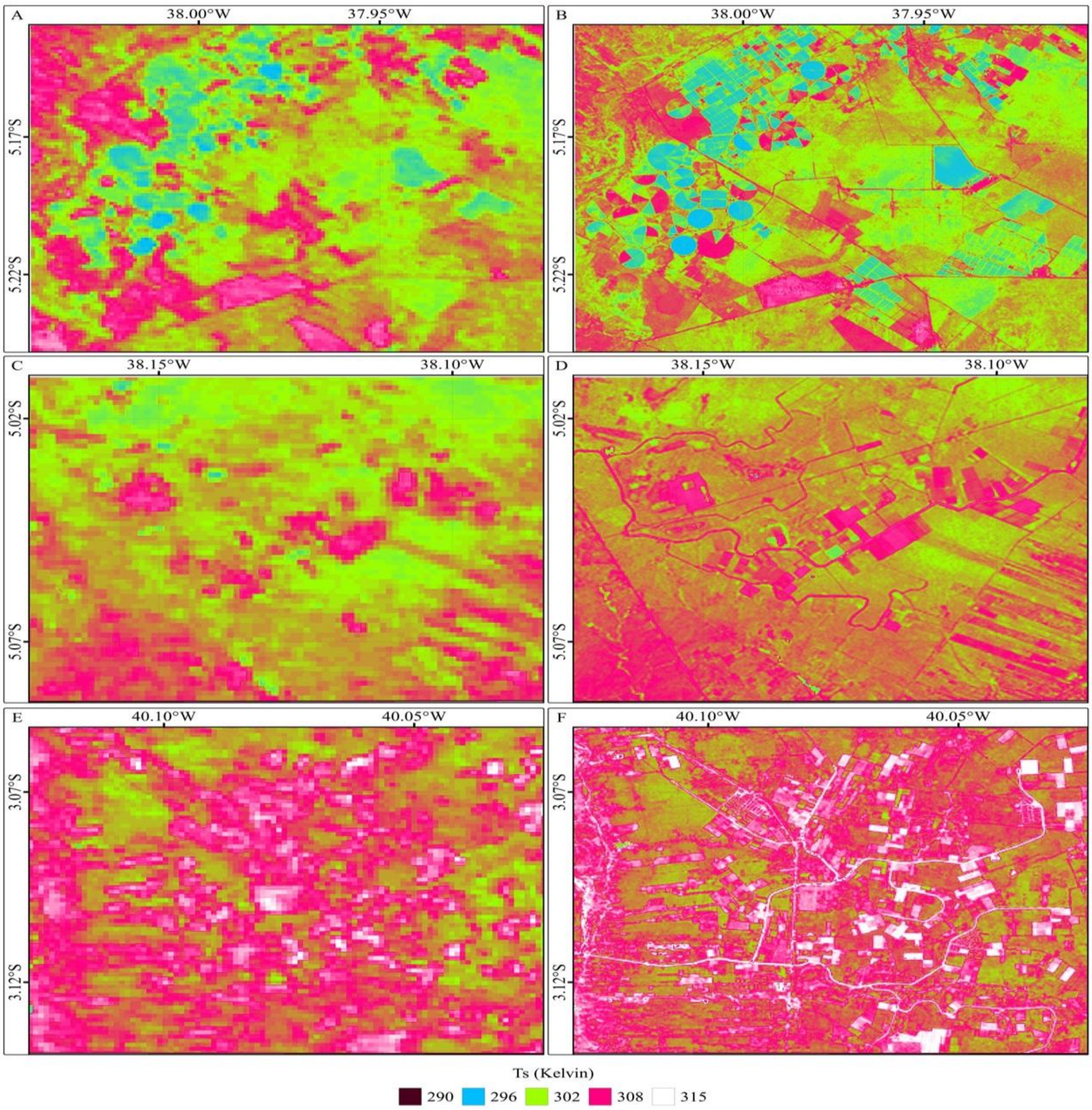

Figure 3. Spatial distribution of Ts-A, TS-Refined-B for DIJA, Ts-C, TS-Refined-D for DISTAR and Ts-E, TS-Refined-F for DIBAU, for the dates August of 6 and 8, 2006.

Similar research was conducted by Anderson et al. (2004) using the TsHARP algorithm proposed by Kustas et al. (2003) to perform the refinement of Ts banana areas in DIJA.

The authors have shown that an inverse relationship exists between the variables NDVI and Ts, and that they are strongly related to soil cover fraction and evapotranspiration. According to Araujo et al. (2012), while testing three different models for the refinement of Ts, it is noted that any of the methods used generated results similar to what was proposed by Agam et al. (2007), however the author recommends using model two (M2) with linear regression between the average values of NDVI and Ts from NDVI classes grouped in the range of 0.1 because it is a simple method.

This situation confirms the observations of Allen et al. (2010), where the authors found that ET image computed after resampling Ts had less distortion, considering that extrinsic factors such as altitude, precipitation and moisture present little effect.

The use of this technique can provide Ts estimates with more useful resolutions for environmental monitoring in different types of ground cover. This image enhancement technique was unable to recreate variations in surface temperature due to anomalies soil moisture were not determined (ARAUJO et al. 2012).

Analyzing (Figure 4 and Figure 5), we see the significant improvement occurred in the spatial resolution of the images ETrf_Refined in agricultural areas. With refinement and ETrf_Refined image composition, it has become possible to perform a thorough analysis of irrigated areas, which would be practically impossible using only ETrf_coarse image area of reduced dimensions. In this way it can be verified that the evapotranspiration fraction values range from 0.0 in areas with low evaporation rate in red, as the maximum evapotranspiration fraction values can exceed the value of 1.5 in the places indicated with intense green color these values are observed in the villages irrigated with pivot or areas with intense agricultural activity. Statistical analysis was carried out checking the behavior and frequency distribution of evapotranspiration in each of the scenes analyzed by histogram composition (Figurre 5). The procedure consists in converting the digital values of each pixel in text tabular data. After the histogram composition realizes that the frequency distribution of values ETrf_Refined faithfully corresponding with the displayed images.

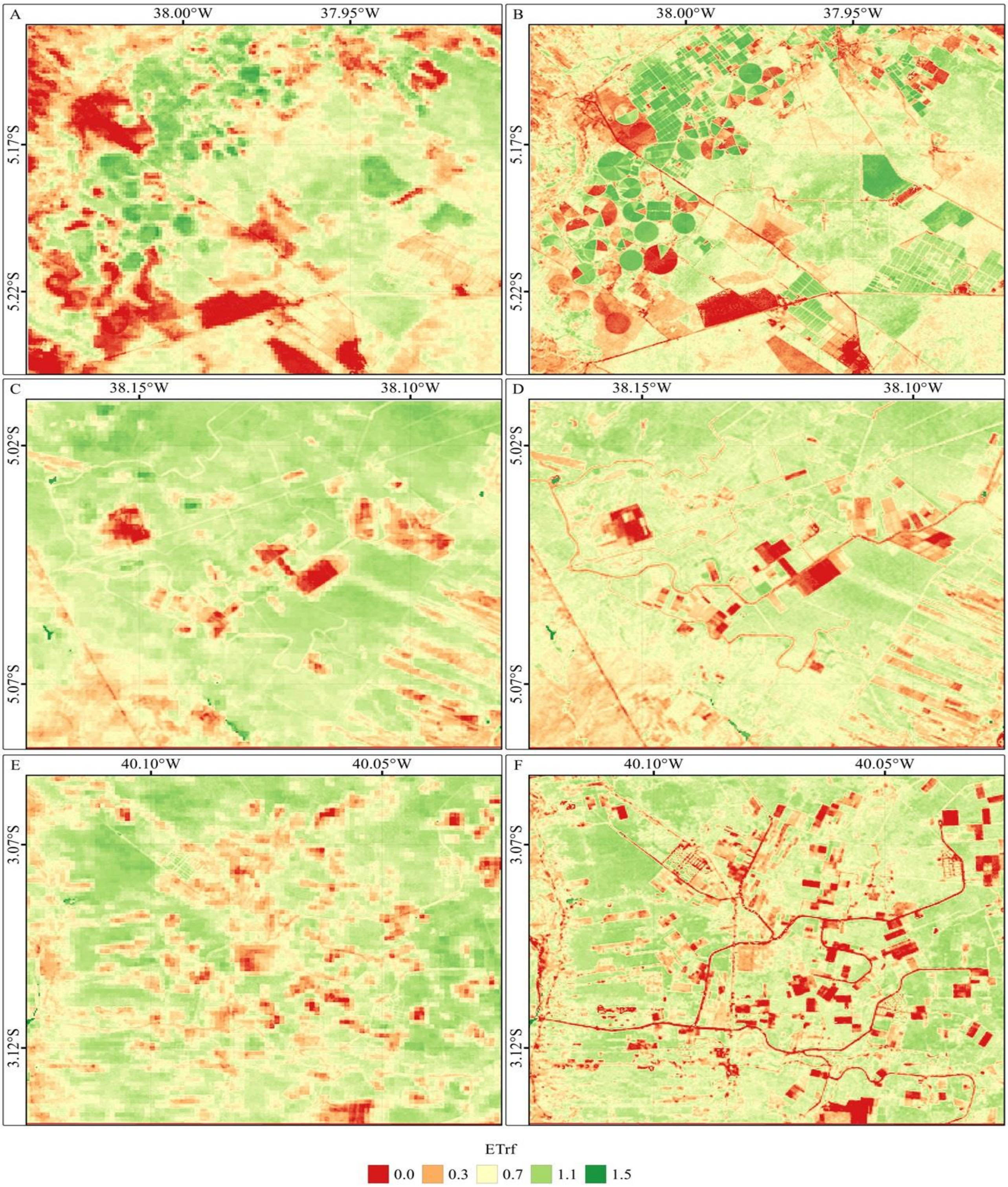

Figure 4. Spatialization of ETrf-Coarse-A, ETrf-Refined-B for DIJA, ETrf-Coarse-C, ETrf-Refined-D for DISTAR and ETrf-Coarse-E, ETrf-Refined-F for DIBAU, for the dates August of 6 and 8, 2006.

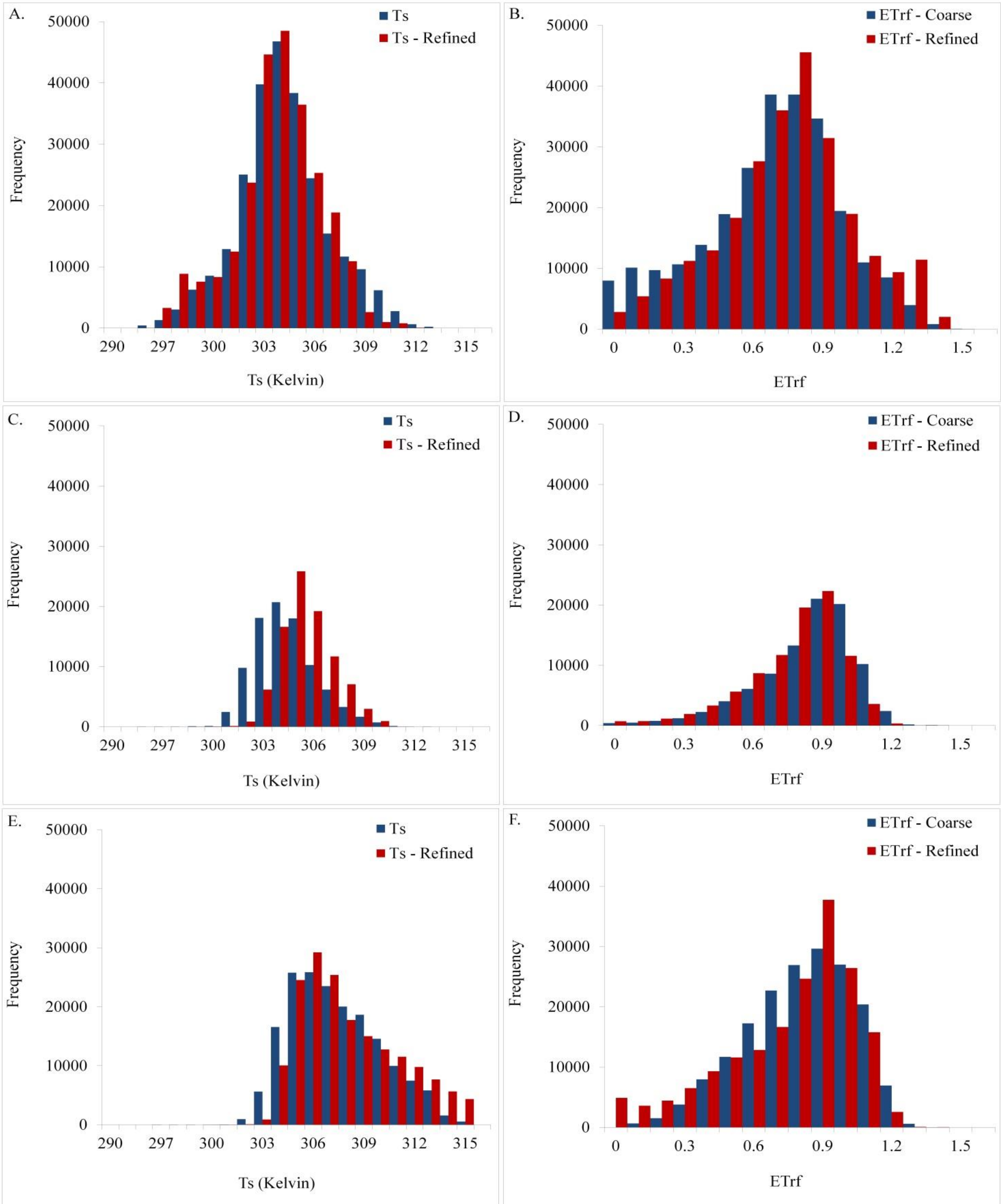

Figure 5. Histograms with the frequency of distribution of values Ts and Ts-Refined-A, ETrf-Coarse and ETrf-Refined-B for DIJA, Ts and Ts-Refined-C, ETrf-Coarse and ETrf-Refined-D for DISTAR, Ts and Ts-Refined-E, ETrf-Coarse and ETrf_Refinada-F for DIBAU, for the day 6 and 8 of August 2006.

Images of ETrf_Refined of irrigated perimeters DISTAR (Figure 4D) and DIBAU (Figure 4F) have similar situations; however, the values of ETrf_Refined related to the scene of DIJA (Figure 4B) shows different behavior compared to the other irrigation districts. It has been found increased lower and mean values, and reduction of the maximum values, compared to the ETrf_coarse image. This behavior may have been influenced by the decline of high Ts values close to irrigated areas on the left bank of the image, given that the vegetation index is higher in these areas and hence boosted the average and maximum values of evapotranspiration, providing a ground cover of view closer to the local reality.

Studies by Allen et al. (2010) in irrigated agricultural areas in the city Kimberly in the US state of Idaho used a similar model to achieve the refinement of the thermal band and get values of evapotranspiration fraction (ETrf_Refined), to estimate the ETrf_Refined. The authors have replaced conventional energy balance variables (Go, H, RN and LET) by variables obtained after refining the thermal band, achieving significant improvement in spatial resolution of actual evapotranspiration images. The refinement of Ts reinforces the need for satellite thermal images with high spatial resolution for better differentiation of changes in land cover (vegetation or agricultural crops) and humidity conditions.

The values obtained for ETrf irrigated agricultural areas vary between 0.8 and 1.4. This ETrf is equivalent to the crop coefficient Kc, thus it can be multiplied by the reference eveapotranspiration, obtained values daily, weekly or monthly, improving the irrigation or water management. The results corroborate to others in literature (FOLHES, 2007; HERNANDEZ et al. 2011; JABOINSKI, 2011; SCHERER-WARREN; RODRIGUES, 2013), in which remote sensing data were used in order to quantify the values of actual evapotranspiration fraction to different cultures among them bananas, beans, corn, soybeans, and sorghum. The maximum observed during the period of harvest crops were evaluated 1.11 (banana), 1.04 (bean), 1.19 (corn), 1.2 (soybean and sorghum). The research was conducted in the states of São Paulo, Mato Grosso, Rio Grande do Sul, and Ceará. The images used covered most months of the second half of the years 2004, 2005 and 2006 (SCHERER-WARREN; RODRIGUES, 2013).

This work achieved the refinement of the thermal band, based on the correlation between NDVI and Ts variables to generate a new image of Ts with spatial resolution of 30m x 30m pixels, maintained most of the original information.

As demonstrated in the research, the monitoring of agricultural irrigated areas through remote sensing, based on refinement of Ts images, tends to generate highly valuable information for managers and irrigators. Among them we can mention obtaining the evapotranspiration fraction (ETrf) and or coefficient of cultivation (Kc) and consequently the advisory use of irrigation water. This information adds to that the farmer can follow the development of culture by providing the conditions necessary for their full development.

CONCLUSIONS

It is evident that the refinement of the thermal band contributes considerably, improving the spatial resolution of Ts images and ETr by 16 times, so that the values are equivalently distributed between areas that have reduced dimensions, providing the construction of a true scene of the field reality. The refinement of the thermal band presents itself as an extremely important tool for performing estimation of actual evapotranspiration values or Kc, serving as a reference to optimize the water requirement calculation on a regional basis, contributing to activities directed at environmental level, resource management water, and agriculture in general.

REFERENCES

AGAM, N.; KUSTAS, W. P.; ANDERSON, M. C.; LI, F.; NEALE, C. M. U. A. A vegetation index is based spatial sharpening technique of thermal imagery. **Remote Sensing of Environment**, v. 107, n. 4, p. 545-558, 2007. https://doi.org/10.1016/j.rse.2006.10.006

ALLEN, R. G.; ROBISON, C. W.; GARCIA, M.; KJAERSGAARD, J. **Enhanced**

resolution of evapotranspiration by the sharpening band Landsat thermal, 3793 N. 3600 E, Kimberly: University of Idaho, 2008.
ALLEN, R.; IRMAK, A.; TREZZA, R.; HENDRICKX, J. M. H.; BASTIAANSSEN, W.; KJAERSGAARD, J. Satellite-based estimation using SEBAL in agriculture and METRIC. **Hydrological Processes**, v. 25, n. 26, p. 4011-4027, 2011. https://doi.org/10.1002/hyp.8408

ALLEN, R.; TASUMI, M.; TREZZA, R. Satellite-Based Energy Balance for Mapping Evapotranspiration with Internalized Calibration (METRIC) -Model. **Journal of Irrigation and Drainage Engineering**, v. 133, n. 4, p. 380-394, 2007. https://doi.org/10.1061/(ASCE)0733-9437(2007)133:4(380)

ALLEN, R.G.; TASUMI, M.; TREZZA, R.; KJAERSGAARD, J. **Mapping evapotranspiration at high resolution, manual application for Landsat satellite imagery.** Version 2.0.7. Kimberly: University of Idaho. 2010.

ANDERSON, M. C.; NEALE, C. M. U.; LI, F.; NORMAN, J. M.; KUSTAS, W. P.; JAYANTHI, H.; CHAVEZ, J. Upscaling ground observations of vegetation water content, canopy height, leaf area index and SMEX02 During aircraft and using Landsat imagery. **Remote Sensing of Environment**, v. 92, n. 1, p. 447-464, 2004. https://doi.org/10.1016/j.rse.2004.03.019

ARAUJO, A. O.; MENDONCA, L. A. R.; LIMA, M. G. S. L.; FEITOSA, N.; SILVA, F. J. A.; NESS, R. L. L.; FRISCHKORN, H.; SIMPLÍCIO, A. A. F.; KERNTOPF, M. R. Refinement thermal 5- Landsat TM images based on NDVI classes. **Journal of Meteorology**, v. 27, n. 4, p. 484-490, 2012.

BASTIAANSSEN, W. G. M.; NOORDMAN, E. J. M.; PELGRUM, H.; DAVIDS, G.; THORESON, B. P.; ALLEN, R. G. SEBAL Model with Remotely Sensed Data to Improve Water-Resources Management under Current Conditions Field. **Journal of Irrigation and Drainage Engineering**, v. 131, n. 1, p. 85-93, 2005. https://doi.org/10.1061/(ASCE)0733-9437(2005)131:1(85)

CAITANO, R. F.; LOPES, F. B.; TEIXEIRA, A. dos S. Estimativa da aridez no Estado do Ceará usando Sistemas de Informação Geográfica. *In:* Simpósio Brasileiro de Sensoriamento Remoto-SBSR, 15., 2011, Curitiba. **Anais...** Curitiba: INPE, 2011. p. 8904.

CHANDER, G., MARKHAM, B.L., HELDER, D.L. Summary of current radiometric calibration coefficients for Landsat MSS, TM, ETM+, and EO-1 ALI sensors. **Remote Sensing of Environment,** v.113, p. 893–903, 2009. https://doi.org/10.1016/j.rse.2009.01.007

CLAVERIE, M.; VERMOTE, E. F.; FRANCH, B.; MASEK, J. G. Evaluation of the Landsat TM 5 and Landsat-7 ETM + surface reflectance products. **Remote Sesing of Environment**, v. 169, n. 1, p. 390-403, 2015. https://doi.org/10.1016/j.rse.2015.08.030

COELHO, A. P. ROSALEN, D. L. FARIA, R. T. Vegetation indices in the prediction of biomass and grain yield of white oat under irrigation levels. **Pesquisa Agropecuaria Tropical**, v. 48, n. 2, p. 109-117, 2018. http://dx.doi.org/10.1590/1983-40632018v4851523

EBC – Empresa Brasil de Comunição. **Agriculture is who spends more water in Brazil and worldwide**. Available in: http://www.ebc.com.br/noticias/internacional/2013/03/agricultura-e-quem-mais-gasta-agua-no-brasil-e-no-mundo. December 12. 2016.

FOLHES, M. T. **Modeling evapotranspiration for water management in irrigated perimeter based on remote sensing**. 2007. 186 f. Doctoral Thesis (Doctorate in Remote Sensing) - National

Institute of Space Research, São José dos Campos.

HERNANDEZ, F. B. T.; NEALE, C. M. U.; TAGHVAEIAN, S.; TEIXEIRA, A. H. C. **Preliminary evaluation of SEBAL model to estimate the spatial distribution of evapotranspiration in irrigated areas in northwestern São Paulo**. In: XV Brazilian Symposium on Remote Sensing - SBSR, 2011, Curitiba, 2011.

JABOINSKI, F. R. **MODIS products Assessment for applications in the estimation of biophysical parameters of the soybean crop in the state of Rio Grande do Sul Federal University of Rio Grande do Sul**. 2011. 89 f. Master Thesis (Master in Remote Sensing) – Federal Uiversity of Rio Grande do Sul, Porto Alegre.

KUSTAS, W. P.; NORMAN, J. M.; ANDERSON, M. C.; FRENCH, A. N. Estimating subpixel surface temperature and energy fluxes from the vegetation index-radiometric temperature relationship. **Remote Sensing of Environment**, v. 85, n. 1, p. 429-440, 2003. https://doi.org/10.1016/S0034-4257(03)00036-1

MACHADO, C. C.; SILVA, B. D.; ALBUQUERQUE, M. B.; GALVÍNCIO, J. D. Estimated energy balance using TM images - Landsat 5 and SEBAL the south coast of Pernambuco. **Journal of Meteorology**, v. 29, n. 1, p. 55-67, 2014.

SCHERER-WARREN, M.; RODRIGUES, L. N. **Estimation of evapotranspiration by remote sensing: procedures and applications central pivot**. EMBRAPA cerrado: Planaltina-DF, 2013. 35 p. (R & D Bulletin).

SPILIOTOPOULOS, M.; HOLDON, N. M.; LOUKAS, A. Mapping evapotranspiration coefficients in the temperate maritime climate using the model and METRIC Landsat TM. **Water-Open Access Journal**, v. 9, n. 1, p. 1-15, 2017. https://doi.org/10.3390/w9010023

TUCKER, C. J. Red and photographic infrared linear combinations monitoring vegetation. **Journal of Remote Sensing Environment**, v. 8, n. 2, p.127-150, 1979. https://doi.org/10.1016/0034-4257(79)90013-0

ZHOU, X.; HUANG, W.; KONG, W.; YE, H.; LUO, J.; CHEN, P. Remote estimation of canopy nitrogen content in winter wheat using airborne hyperspectral reflectance measurements. **Advances in Space Research**, v. 58, n. 9, p. 1627-1637, 2016. https://doi.org/10.1016/j.asr.2016.06.034